Spectrochimica Acta Part A: Molecular and Biomolecular Spectroscopy 263 (2021) 120173

Contents lists available at ScienceDirect

Spectrochimica Acta Part A: Molecular and Biomolecular Spectroscopy

journal homepage: www.elsevier.com/locate/saa

A reversible coumarin-based sensor for intracellular monitoring cysteine level changes during Cu^{2+}-induced redox imbalance

Jianbin Chao [a,*], Jiamin Zhao [a,b], Jinping Jia [a], Yongbin Zhang [c], Fangjun Huo [c], Caixia Yin [d,*]

[a] Scientific Instrument Center, Shanxi University, Taiyuan 030006, China
[b] School of Chemistry and Chemical Engineering, Shanxi University, Taiyuan 030006, China
[c] Research Institute of Applied Chemistry, Shanxi University, Taiyuan 030006, China
[d] Key Laboratory of Chemical Biology and Molecular Engineering of Ministry of Education, Institute of Molecular Science, Shanxi University, Taiyuan 030006, China

HIGHLIGHTS

- A reversible probe (**HNA**) was prepared based on coumarin.
- **HNA** exhibited high response speed and low detection limit for Cys/Hcy.
- **HNA** can evaluate the effect of copper (II)-induced oxidative stress on Cys levels in living cells and zebrafish.

GRAPHICAL ABSTRACT

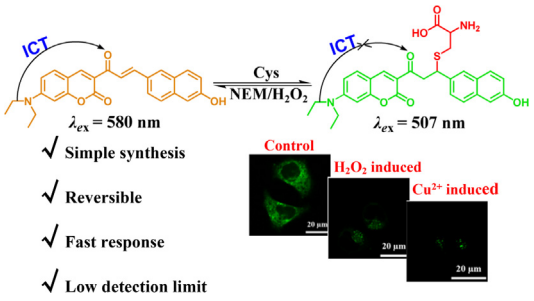

ARTICLE INFO

Article history:
Received 17 June 2021
Received in revised form 6 July 2021
Accepted 7 July 2021
Available online 14 July 2021

Keywords:
Coumarin
Cys/Hcy
Cu^{2+}
Redox imbalance
Bioiaging

ABSTRACT

Biological thiols are crucial small molecule amino acids widely existing in cells, which play indispensable roles in maintaining redox homeostasis of living systems. Owing to their abnormal levels have close relation with many diseases, thus, developing more convenient, rapid and practical in-vivo detection tools is imminent. Herein, a reversible coumarin-based probe (**HNA**) was successfully constructed through a simple two-step synthesis. **HNA** can detect Cys/Hcy with high response speed and desirable selectivity based on Michael addition recognition mechanism. Free **HNA** has an orange emission at 580 nm, but after addition of Cys/Hcy, the conjugated structure of probe **HNA** was destroyed by the attack of sulfhydryl, resulting in a new green emission at 507 nm. Further, **HNA** has been applied to monitor Cys/Hcy in HeLa cells and zebrafish. Notably, **HNA** has also been successfully applied for real-time tracing Cys levels changes in living cells and zebrafish during the imbalance in redox status caused by copper (II). This provides a new strategy for studying the process of oxidative stress in cells.

1. Introduction

Biological thiols, which are widely present in organisms, are the general term for sulfhydryl-containing compounds in organisms. The most representative biological thiols are: cysteine (Cys), homocysteine (Hcy) and glutathione (GSH), which have pivotal functions in physiological activities [1–4]. Among them, Cys possesses the simplest structure and mainly responsible for the regulation of the redox balance of organisms, with an intracellular concentration of 30–200 μmol.L^{-1} [5,6]. Hcy is mainly involved in the regulation of cell homeostasis, and its intracellular concentration is as low as 5–15 μmol.L^{-1} [7,8]. High intracellular concentration of GSH (1–10 mmol.L^{-1}) is an important biochemical defense system in organisms [9,10]. Aberrant levels of biological thiols in cells may cause various health problems [11–15]. High

* Corresponding authors.
E-mail addresses: chao@sxu.edu.cn (J. Chao), yincx@sxu.edu.cn (C. Yin).

https://doi.org/10.1016/j.saa.2021.120173
1386-1425/

concentration of Cys can cause cardiovascular and neurotoxic diseases, while low concentration is closely related to slow growth, drowsiness, liver injury, skin lesions, fat loss and weakness [16–20]. Studies have revealed that Hcy is a hazard element for angiocardiopathy, inflammation, osteoporosis, and mental diseases such as Alzheimer's disease and schizophrenia [21–25]. The abnormal level of GSH is closely related to cancer, neurodegenerative disease and cardiovascular disease [26–30]. Therefore, there are highly required for more available tools to further understand the relevant functions of biological thiols in human physiology and pathology.

Compared with the previous detection methods for biological thiols [31–33], non-invasive fluorescence probes have aroused wide interest on account of their advantages of simple synthesis, easy to operate, high sensitivity and real-time detection. For this, many fluorescent probes with excellent performance have been developed to identify thiols. However, since the three thiols possess similar molecular structures, it is still difficult to develop effective probes to distinguish them at the same time. Nevertheless, some research groups have successfully developed a few promising probes for discrimination of these three thiols. For instance, Li [34] prepared a dual-site sensor for differentiation of Cys, Hcy and GSH. Ren [35] developed a red-emitting probe to detect Cys/Hcy and GSH. Fu [36] designed three sensors for identification of Cys and GSH.

To our knowledge, coumarin dyes have the advantages of easy modification, large stokes shift and stable optical properties [37–39]. Given these, herein, we constructed a reversible coumarin-based probe (**HNA**) through a simple two-step synthesis. **HNA** exhibited high response speed, desirable selectivity and low detection limits for Cys/Hcy detection. After addition of Cys/Hcy, the carbon-carbon double bond in the α,β-unsaturated ketone structure was nucleophilically attacked by sulfhydryl, resulting in the destruction of the conjugate structure of **HNA**, the emission peak at 580 nm shifted to 507 nm, and green fluorescence was released. Further, **HNA** has been used for imaging Cys and Hcy in HeLa cells and in vivo. More interestingly, we further used **HNA** to monitor Cys levels changes in HeLa cells and zebrafish during the imbalance in redox status caused by copper (II).

2. Experimental section

2.1. Synthesis of the probe HNA

Compound 1 (1 mmol, 0.259 g), 6-hydroxy-2-naphthaldehyde (1 mmol, 0.172 g) were dissolved in anhydrous ethanol (10 mL), then 150 μL piperidine was added. After refluxing for 36 h, the solvent was evaporated and the crude product was further purified by column chromatography (EtOAc/PE = 1/1, v/v) to get a red solid (0.149 g, 36%) (Scheme 1). ^{1}H NMR (600 MHz, DMSO d_6) δ 10.05 (s, 1H), 8.62 (s, 1H), 8.10 (s, 1H), 8.00 (d, J = 15.6 Hz, 1H), 7.82 (dd, J = 22.3, 12.1 Hz, 2H), 7.75 (t, J = 23.6 Hz, 2H), 7.71 (d, J = 8.8 Hz, 1H), 7.16–7.12 (m, 2H), 6.82 (d, J = 8.1 Hz, 1H), 6.63 (s, 1H), 3.51 (d, J = 6.5 Hz, 4H), 1.16 (t, J = 6.4 Hz, 6H). ^{13}C NMR (150 MHz, DMSO d_6): δ 185.88, 160.46, 158.68, 157.37, 153.44, 148.79, 143.12, 136.25, 132.80, 131.01, 130.88, 129.85, 127.98, 127.39, 124.61, 124.09, 119.79, 116.19, 110.69, 109.54, 108.41, 96.40, 44.93, 12.85. HR-MS: m/z calculated for $C_{26}H_{23}NNaO_4$ $[M + Na]^+$: 436.15248, found: 436.15138.

2.2. Optical properties

Probe **HNA** (0.0016 g) was dissolved in DMSO to prepare a stock solution (2 mM). Stock solutions of Cys, Hcy, other amino acids and ions (0.01 M) were prepared in deionized water. All spectroscopy experiments were tested in PBS/DMSO (v/v, 6/4, pH 7.4) system. HeLa cells and zebrafish (4-day-old) were used for bio-imaging studies and the specific culture methods are described in the supporting information.

3. Results and discussion

3.1. Spectral properties

First, we studied the absorption spectrum of **HNA** to Cys in the test system (Fig. 1a). After continuously adding Cys (0–400 μM), the absorption at 480 nm synchronously weakened and blue shifted to 460 nm, which corresponded to the destruction of conjugated structure. Subsequently, the fluorescence spectrum was measured (Fig. 1b), the probe itself had an emission peak at 580 nm, but when Cys was added, a new emission peak appeared at 507 nm and steadily enhanced. The fluorescence spectrum of **HNA** titrated with Hcy was similar to that of Cys (Fig. S1). All these changes were caused by the Michael addition reaction between the sulfhydryl and the double bond, which destroyed the conjugation structure of the probe **HNA**. In addition, we found that the fluorescence intensity was linear with Cys/Hcy concentrations at a wide range of 0–275 μM and 0–325 μM, respectively (R^2 = 0.9993 for Cys and 0.9999 for Hcy) (Fig. 1c). The calculated detection limit of Cys was 8.4 nM, and Hcy was 8.2 nM on the basis of IUPAC recommendation (CDL = 3Sb/m). These results suggested that **HNA** was a reliable tool for distinguishing Cys/Hcy from GSH.

3.2. Kinetic study and reversibility of probe HNA

Then, the kinetics of the **HNA-**Cys/Hcy system was investigated. As illustrated in Fig. 2 and Fig. S2, the fluorescence of **HNA** at 507 nm remained almost unchanged during the whole test, suggesting that the probe **HNA** was stable. However, after addition of 400 μM Cys/Hcy, a significant enhancement in fluorescence was observed at 507 nm, and reached a maximum in a short time. This denoted that **HNA** is a rapid tool for detecting Cys/Hcy.

Reversibility is one of the vital parameters to evaluate the performance of probes. For probe **HNA**, we used NEM (thiol blocking

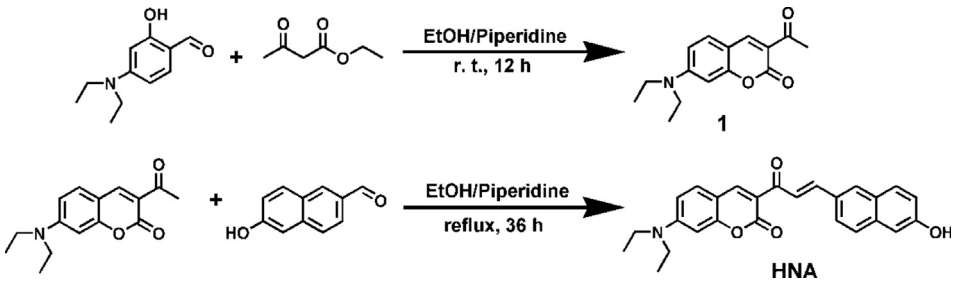

Scheme 1. Synthetic route of probe **HNA**.

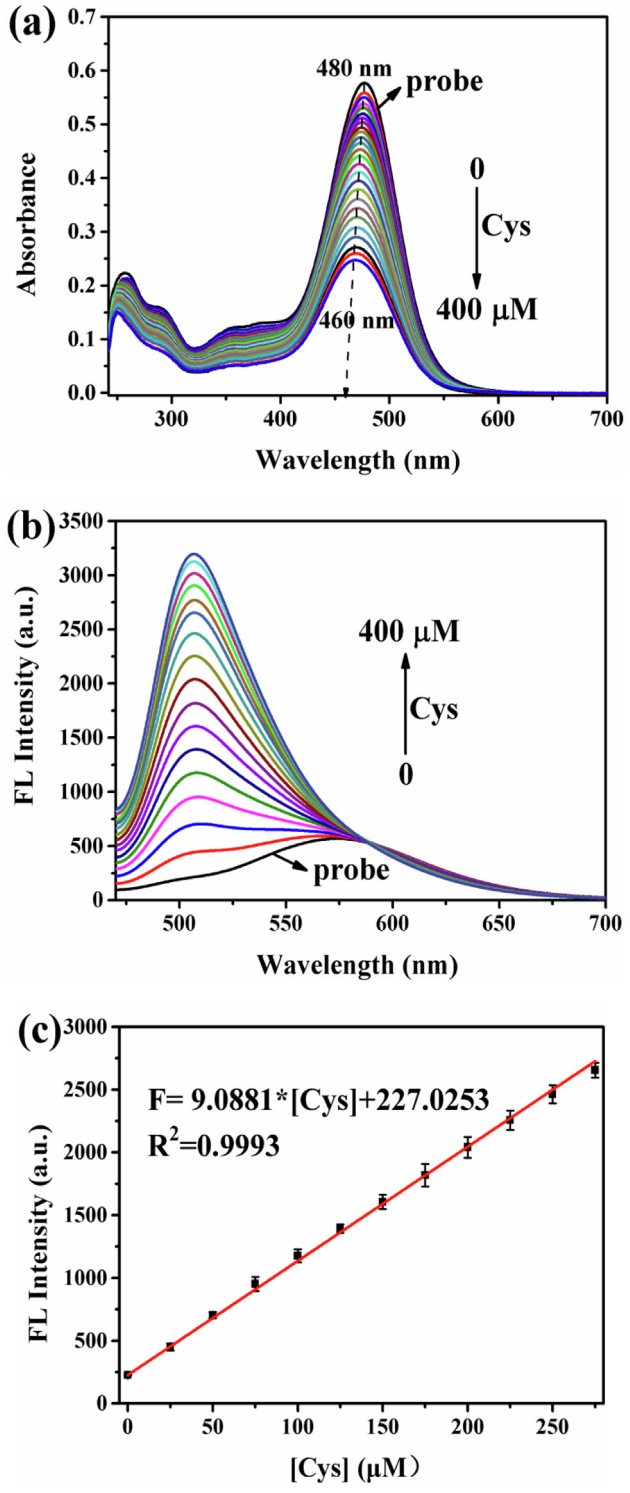

Fig. 1. Spectral response of **HNA** to Cys (PBS/DMSO, v/v, 6/4, pH 7.4). (a) UV absorption spectrum of **HNA** (10 μM) within the Cys range of 0–400 μM; (b) Fluorescence spectrum of **HNA** (10 μM) within the Cys range of 0–400 μM; (c) Linear fit within the Cys range of 0–275 μM. λ_{ex} = 460 nm, slit: 5/5 nm.

agent) and H_2O_2 (a representative ROS that can consume Cys) as inducible factors to study its reversibility (Scheme 2). From the UV absorption spectrum in Fig. 3, we found that free **HNA** had a strong absorption at 480 nm, after addition of 400 μM Cys, the absorption decreased and shifted to 460 nm. However, when NEM and H_2O_2 (400 μM) were added to the above solution

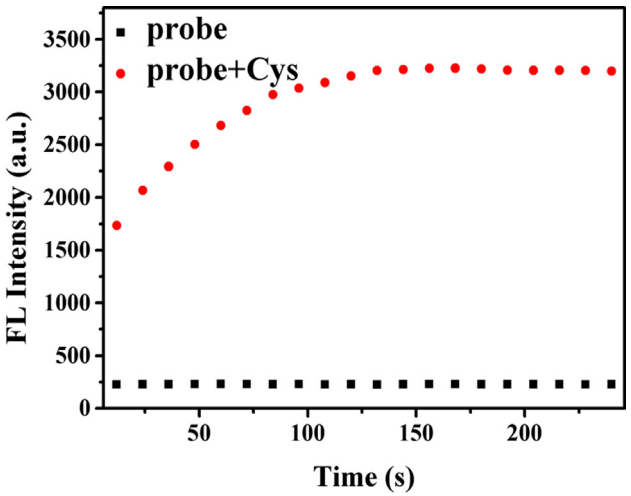

Fig. 2. Kinetics study of **HNA** (10 μM) and **HNA**-Cys system.

respectively, the absorption peak returned to 480 nm, and the absorption intensity was slightly lower than that of adding **HNA** alone. Additionally, we also studied this property through cyclic addition of Cys and NEM/H_2O_2 in the probe solution. As shown in Fig. 4, through five experimental cycles, the fluorescence intensity has undergone a small and non-negligible change. All these hinted that the probe **HNA** has good reversibility and can also be used to evaluate the redox kinetics of Cys and H_2O_2.

3.3. Selectivity, interference and pH experiments

To evaluate the desirable selectivity of **HNA** to Cys/Hcy, we investigated the changes in fluorescence intensity in the presence of common amino acids (Ala, Asp, Arg, Thr, Leu, Tyr, Glu, Ser, His, Trp, Val, Phe, Pro, Gly, Lys, Ile, Gln, Asn, Met) and ions (SO_4^{2-}, SO_3^{2-}, HS^-, $S_2O_3^{2-}$, NO_3^-, CO_3^{2-}, NO_2^-, Cl^-, Br^-, I^-, Ac^-, CrO_4^{2-}, K^+, Fe^{2+}, Mg^{2+}, Na^+, Cu^{2+}, Mn^{2+}, Pb^{2+}, Co^{2+}, Hg^{2+}, Cr^{3+}, NH_4^+). As depicted in Fig. 5a, after addition of 400 μM interfering substances, the fluorescence intensity at 507 nm remained almost unchanged. Further, interference experiments were also performed in the test system, in the presence of these interfering substances (400 μM), the fluorescence intensity of **HNA**-Cys/Hcy system did not change significantly (Fig. 5b, c). All these confirmed that **HNA** can specifically identify Cys/Hcy in complex samples.

In addition, the pH-dependent experiments of **HNA** and **HNA**-Cys/Hcy system were also performed (Fig. 6). The probe **HNA** itself exhibited excellent stability at pH 2.0–10.0. After 400 μM Cys/Hcy was added, obvious fluorescence enhancement was observed at pH 4.0–10.0, and the peak of fluorescence intensity appeared at pH = 7.4. The above facts demonstrated that **HNA** was capable of well applied to detect Cys/Hcy in physiological environment.

3.4. Response mechanism

We proposed that the response mechanism of **HNA** with Cys/Hcy was attributed to Michael addition reaction. As described in Scheme 3, upon addition of Cys/Hcy, the carbon–carbon double bond in the α,β-unsaturated ketone structure was nucleophilic attacked by the sulfhydryl, so that the conjugate structure of the probe **HNA** was broken, the ICT process was changed, and the emission peak at 580 nm shifted to 507 nm, strong green fluorescence was released. Further, this assumption has been verified by mass spectrometry and ^1H NMR titration. The *m*/*z* peaks were observed at 557.17087, 571.18633 (calculated: 557.17223,

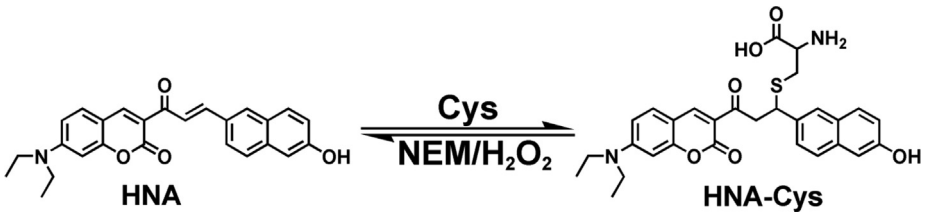

Scheme 2. The possible reversible mechanism between NEM/H_2O_2 and Cys.

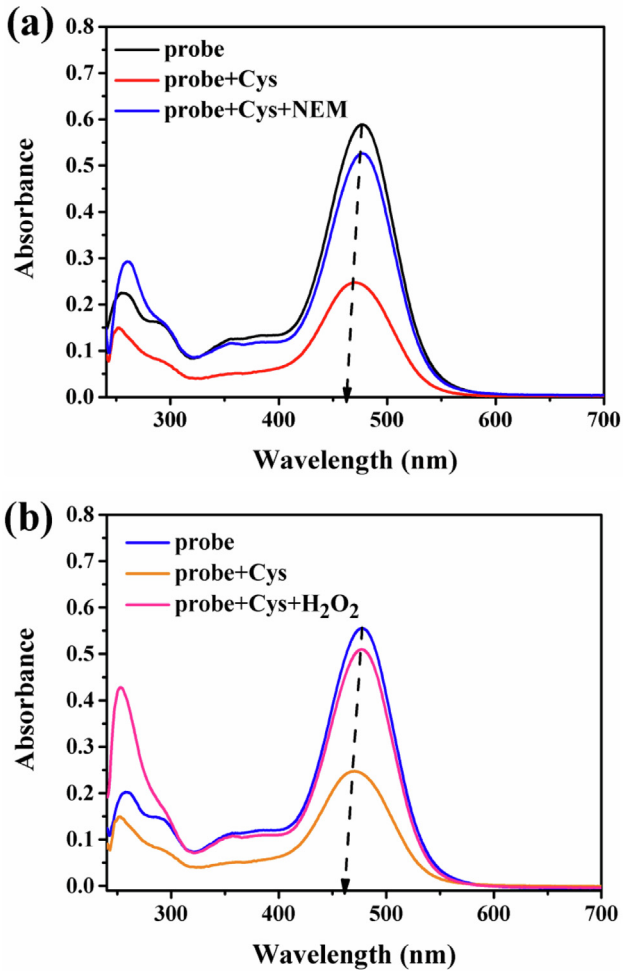

Fig. 3. UV absorption spectra of **HNA** after adding Cys (400 μM) and NEM(a)/H_2O_2(b) (400 μM) in sequence.

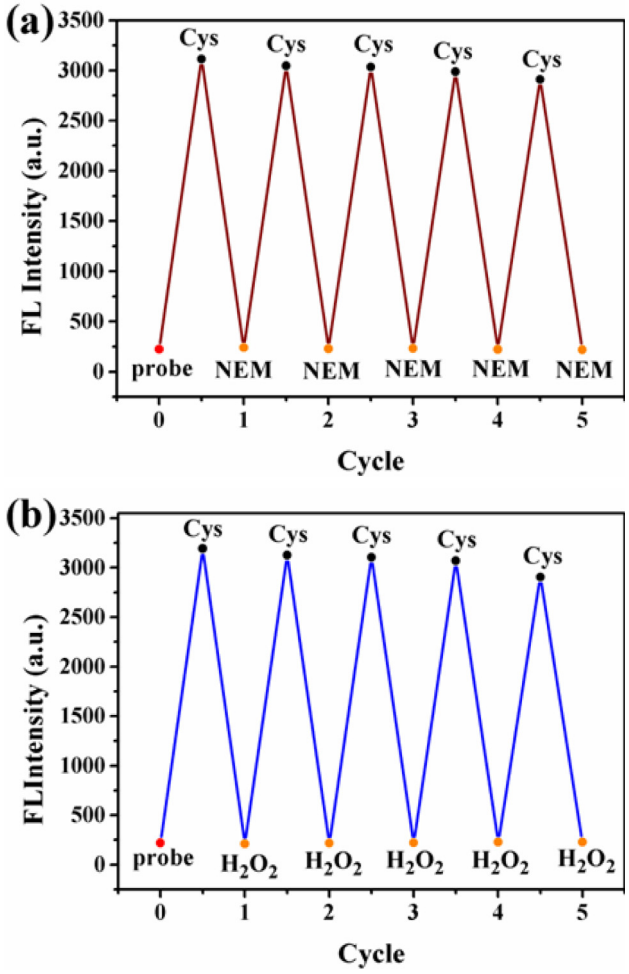

Fig. 4. Reversible study of **HNA** (10 μM) by adding Cys (400 μM) and NEM (a)/H_2O_2 (b) (400 μM) cyclically.

571.18788). After ^{1}H NMR titration, the characteristic signal of the double bond in **HNA** at δ 7.8 (a/c), δ 8.0 (b/d) almost disappeared and new peaks appeared at δ 4.59, 4.03 and 3.76 for Cys, δ 4.55 and 3.73 for Hcy, corresponding to the generated CH and CH_2 protons.

3.5. HeLa cells imaging

Encouraged by the superior optical properties of **HNA**, we further applied it to cell imaging. As described in Fig. 7, after treatment of HeLa cells with **HNA** (10 μM, 10 min), the green channel exhibited weak fluorescence. As a control, NEM-treated cells were further incubated with **HNA** (10 μM, 10 min), and weak orange fluorescence was clearly observed, while no green fluorescence was observed. Next, **HNA** was used for detecting exogenous Cys/Hcy. NEM-treated cells were further incubated with Cys/Hcy (200 μM, 10 min) and **HNA** (10 μM, 10 min), the green channel displayed intense florescence. These results demonstrated the ability of **HNA** for imaging Cys/Hcy in living cells.

Oxidative stress (OS) is a state of imbalance between oxidation and antioxidation, that is, redox imbalance, which is considered to be an important factor leading to aging and diseases [40,41]. Cysteine, as a potential endogenous antioxidant, plays a vital role in retaining cell redox homeostasis. Moreover, related papers pointed out that copper (II) stimulation can induce cells to produce ROS, and the generated reactive oxygen species further undergo redox reactions with Cys, resulting in a significant decrease in the intracellular Cys content [42–44]. Since the intracellular content of Hcy is much lower than that of Cys, under this premise, redox balance was altered by H_2O_2/Cu^{2+}, and the changes of Cys levels in HeLa

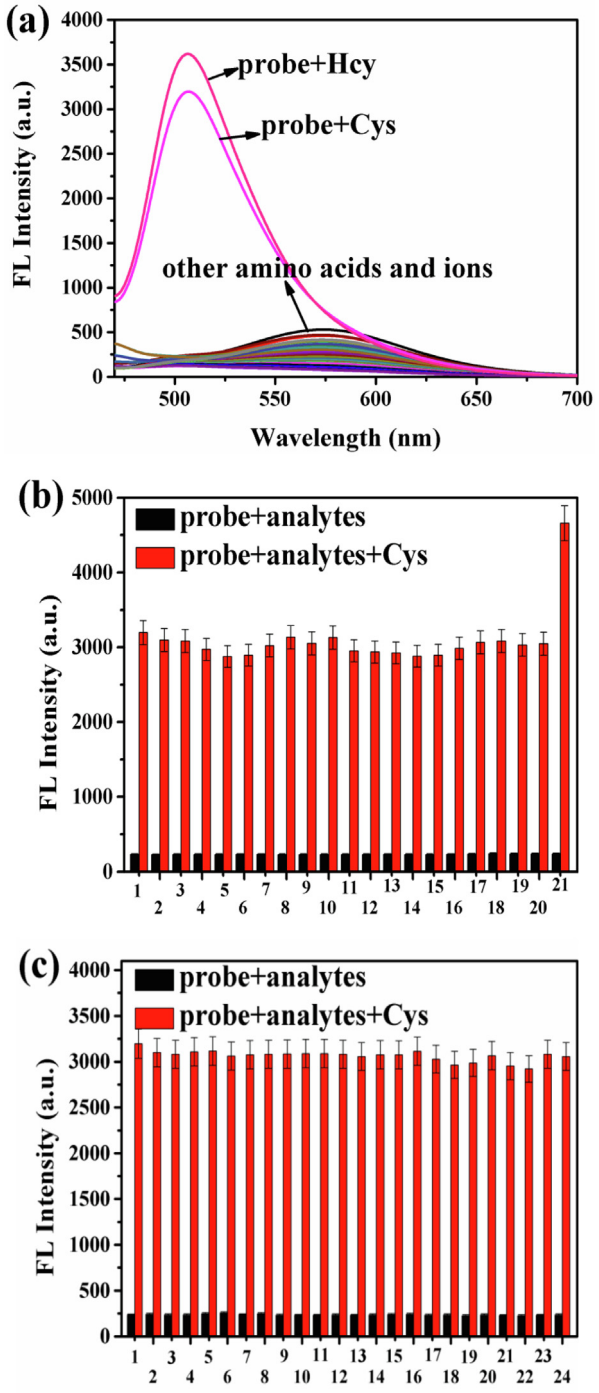

Fig. 5. The specific response of **HNA** to Cys. (a) Fluorescence spectrum of **HNA** (10 μM) after adding various amino acids and ions (400 μM); (b) Fluorescence intensity of **HNA** (10 μM) for other amino acids in the presence and absence of 400 μM Cys (1.blank, 2.Ala, 3.Asp, 4.Arg, 5.Thr, 6.Leu, 7.Tyr, 8.Glu, 9.Ser, 10.His, 11. Trp, 12.Val, 13.Phe, 14.Pro, 15.Gly, 16.Lys, 17.Ile, 18.Gln, 19.Asn, 20.Met, 21.Hcy); (c) Fluorescence intensity of **HNA** for various ions in the presence and absence of 400 μM Cys (1.blank, 2.SO_4^{2-}, 3.SO_3^{2-}, 4.HS^-, 5.$S_2O_3^{2-}$, 6.NO_3^-, 7.CO_3^{2-}, 8.NO_2^-, 9.Cl^-, 10. Br^-, 11.I^-, 12.Ac^-, 13.CrO_4^{2-}, 14.K^+, 15.Fe^{2+}, 16.Mg^{2+}, 17.Na^+, 18.Cu^{2+}, 19.Mn^{2+}, 20. Pb^{2+}, 21.Co^{2+}, 22.Hg^{2+}, 23.Cr^{2+}, 24.NH_4^+). All data were recorded after mixing for 3 min.

cells were investigated through the fluorescence response of **HNA**. As illustrated in Fig. 8, HeLa cells on incubation with **HNA** (10 μM, 10 min) emitted green fluorescence, and the fluorescence intensity

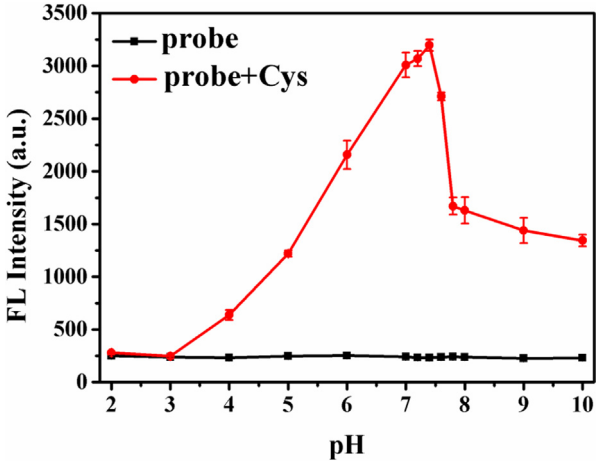

Fig. 6. Fluorescence intensity of **HNA** and **HNA**-Cys system under different pH conditions.

was almost unchanged within 20 min. When the incubation of HeLa cells with **HNA** (10 μM, 10 min) and H_2O_2 (2 mmol/L) successively, the green fluorescence was gradually reduced within 20 min. This implied that the addition of H_2O_2 induced oxidative stress, which consumed Cys in cells. Next, we investigated the effect of Cu^{2+} on the induction of oxidative stress in HeLa cells, using $Cu(NO_3)_2{\cdot}3H_2O$ as the copper source. HeLa cells treated with **HNA** (10 μM, 10 min) and Cu^{2+} (2 mmol/L) sequentially, the intensity of green fluorescence decreased significantly within 20 min. All these results may be due to the fact that HeLa cells produced ROS under the stimulation of copper (II), the generated ROS (similar to H_2O_2) undergo a redox reaction with Cys, thereby reducing the intracellular Cys levels. So the fluorescence intensity of the green channel was gradually weakened.

3.6. Zebrafish imaging

To further evaluate the imaging performance of **HNA** in vivo, we conducted laser confocal microscopy imaging experiments using zebrafish as a model. As illustrated in Fig. 9, after the zebrafish co-incubated with **HNA** (10 μM, 10 min), the green channel showed weak fluorescence. In contrast, NEM-treated zebrafish were further incubated with **HNA** (10 μM, 10 min), and no fluorescence signal was observed in the green channel, but there was fluorescence emission in the orange channel. Then, the zebrafish cleared by NEM (500 μM, 30 min) were further treated with Cys/Hcy (200 μM, 10 min) and **HNA** (10 μM, 10 min), and the green channel showed intense fluorescence. These phenomena suggested the excellent in vivo imaging performance of **HNA**.

In addition, the redox imbalance induced by Cu^{2+} in zebrafish was also evaluated. Zebrafish treated with **HNA** (10 μM, 10 min) and Cu^{2+} (2 mmol/L) sequentially, and the changes in the fluorescence intensity of the green channel were collected over time. From Fig. 10a, we observed that the green fluorescence gradually weakened in 20 min. Similarly, we used H_2O_2 as the representative of reactive oxygen species to study its effect on the redox process in zebrafish (Fig. 10b). After the treatment of zebrafish with **HNA** (10 μM, 10 min) and H_2O_2 (2 mmol/L) separately, we observed that the fluorescence signal of green channel gradually decreased within 20 min. These phenomena indicated that Cu^{2+} can induce the production of ROS in zebrafish, and excessive ROS consumed Cys in zebrafish, resulting in the decrease of green fluorescence.

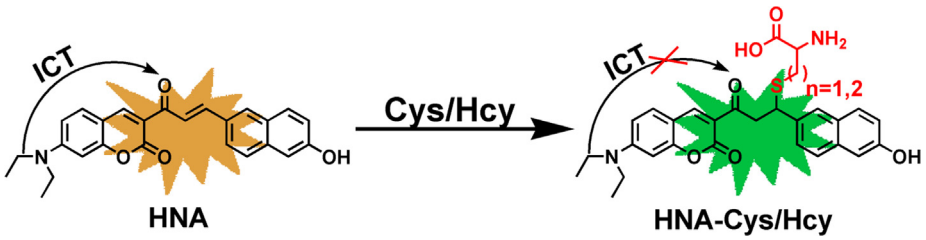

Scheme 3. Proposed reaction process between **HNA** and Cys/Hcy.

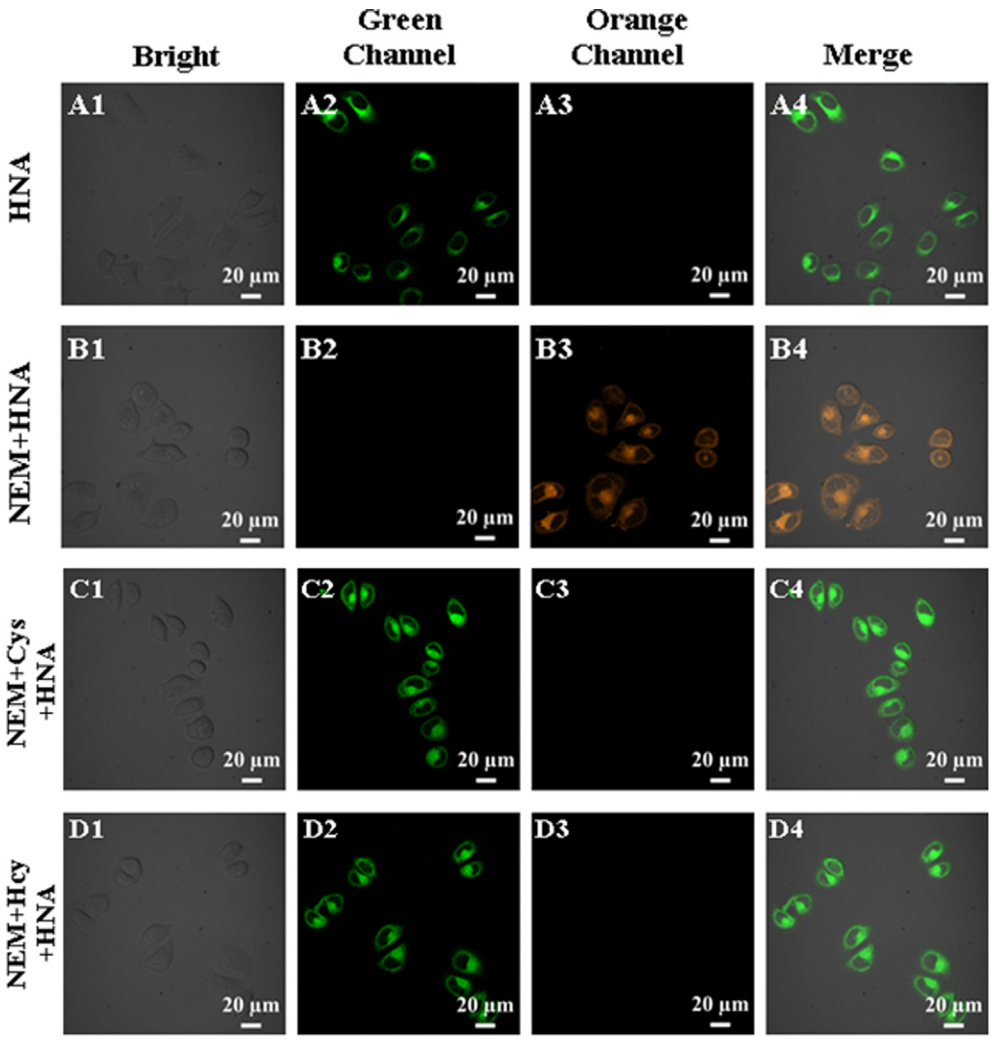

Fig. 7. Imaging of Cys/Hcy in HeLa cells with **HNA**. Orange channel: λ_{em} = 580 ± 30 nm (λ_{ex} = 488 nm); Green channel: λ_{em} = 507 ± 30 nm (λ_{ex} = 458 nm).

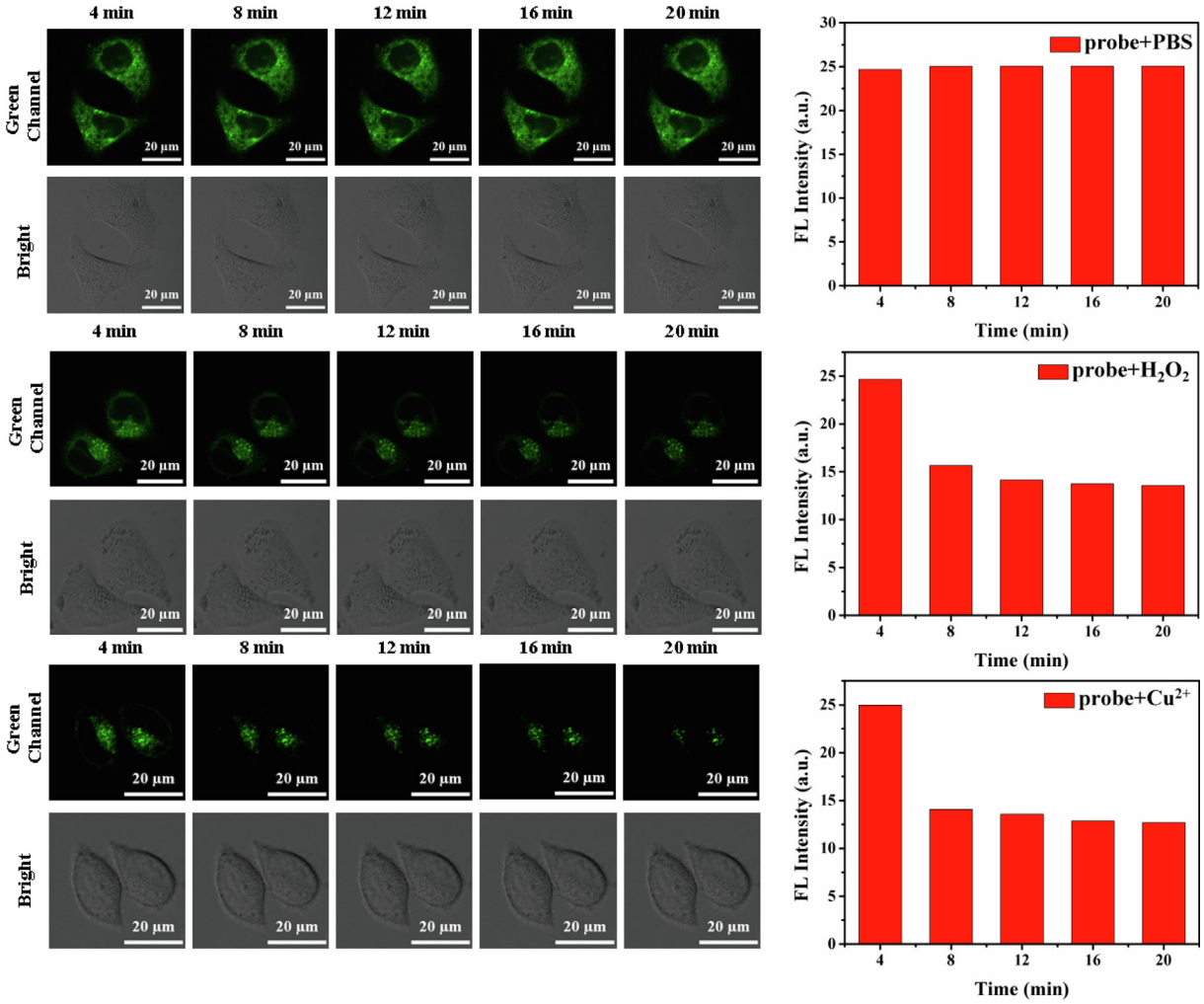

Fig. 8. Time-dependent cell imaging with **HNA** (10 μM) and PBS/H_2O_2/Cu^{2+}. Green channel: λ_{em} = 507 ± 30 nm (λ_{ex} = 458 nm).

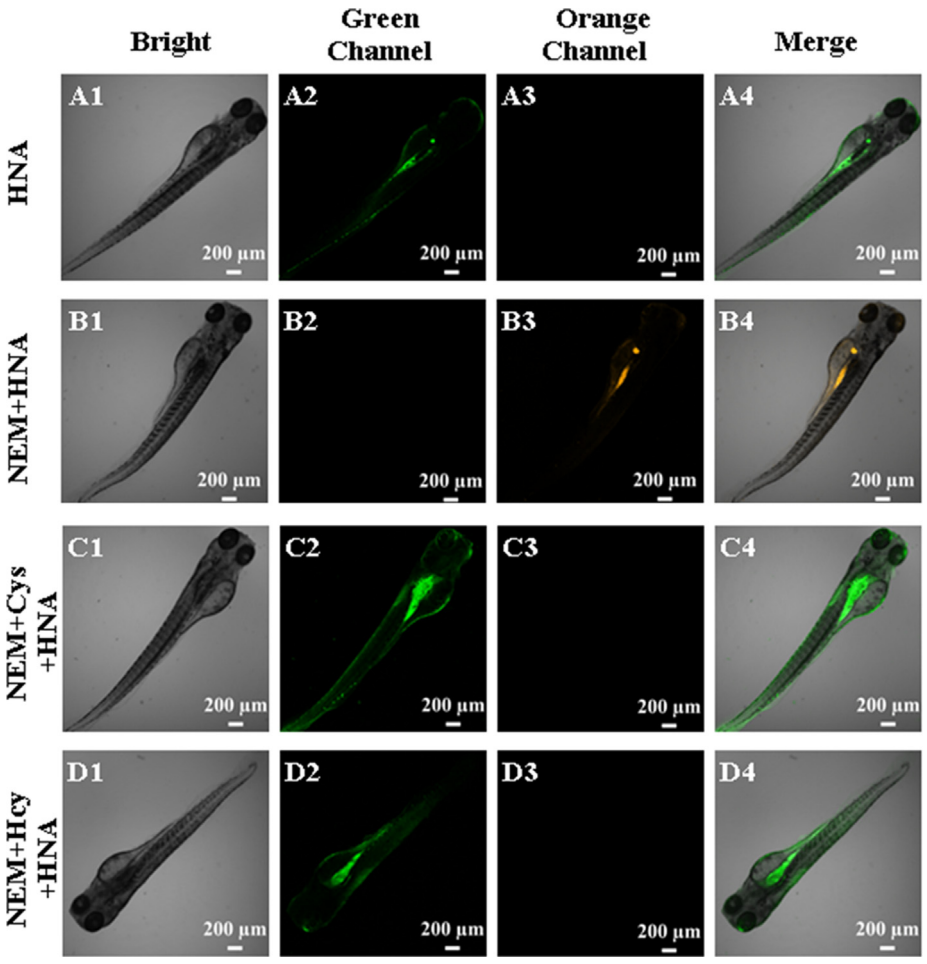

Fig. 9. Imaging of Cys/Hcy in zebrafish with **HNA**. Orange channel: λ_{em} = 580 ± 30 nm (λ_{ex} = 488 nm); Green channel: λ_{em} = 507 ± 30 nm (λ_{ex} = 458 nm).

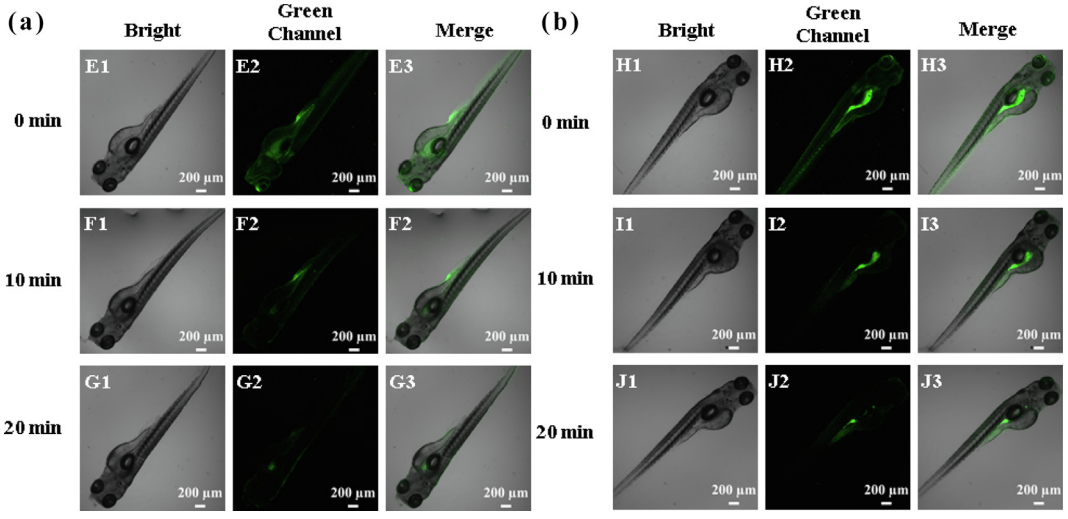

Fig. 10. Time-dependent zebrafish imaging with **HNA** (10 μM) and Cu^{2+} (2 mmol/L) (a)/H_2O_2 (2 mmol/L) (b). Green channel: λ_{em} = 507 ± 30 nm (λ_{ex} = 458 nm).

4. Conclusion

In conclusion, we have employed a reversible coumarin-based sensor (**HNA**) to distinguish Cys/Hcy from GSH based on destruction effect of sulfhydryl on α, β-unsaturated ketone. **HNA** exhibited desirable selectivity, rapid response time and low detection limits for Cys/Hcy detection. Finally, **HNA** was further used for imaging endogenous and exogenous Cys/Hcy in HeLa cells and zebrafish with its good cell permeability and in vivo imaging capabilities. Additionally, it is worth mentioning that **HNA** was also applied to estimate copper (II)-induced redox imbalance in HeLa cells and zebrafish, which will provide the possibility for us to understand the relevant functions of Cys in organisms.

CRediT authorship contribution statement

Jianbin Chao: Conceptualization, Methodology, Supervision. **Jiamin Zhao:** Formal analysis, Investigation, Resources, Data curation, Writing - original draft, Visualization. **Jinping Jia:** Conceptualization, Methodology, Supervision. **Yongbin Zhang:** Conceptualization, Methodology, Supervision. **Fangjun Huo:** Validation, Writing - review & editing. **Caixia Yin:** Validation, Writing - review & editing.

Declaration of Competing Interest

The authors declare that they have no known competing financial interests or personal relationships that could have appeared to influence the work reported in this paper.

Acknowledgements

We thank the National Natural Science Foundation of China (No. 21472118, 21672131), the Program for the Top Young and Middle-aged Innovative Talents of Higher Learning Institutions of Shanxi (No. 2013802), Talents Support Program of Shanxi Province (No. 2014401), Shanxi Province Outstanding Youth Fund (No. 2014021002), Natural Science Foundation of Shanxi Province of China (No. 201701D121018).

Appendix A. Supplementary material

Supplementary data to this article can be found online at https://doi.org/10.1016/j.saa.2021.120173.

References

[1] L.Y. Niu, Y.Z. Chen, H.R. Zheng, L.Z. Wu, C.H. Tung, Q.Z. Yang, Design strategies of fluorescent probes for selective detection among biothiols, Chem. Soc. Rev. 44 (2015) 6143–6160.
[2] W.Q. Chen, H.C. Luo, X.J. Liu, J.W. Foley, X.Z. Song, Broadly applicable strategy for the fluorescence based detection and differentiation of glutathione and cysteine/homocysteine: demonstration in vitro and in vivo, Anal. Chem. 88 (2016) 3638–3646.
[3] M.W. Yang, J.L. Fan, W. Sun, J.J. Du, X.J. Peng, Mitochondria-anchored colorimetric and ratiometric fluorescent chemosensor for visualizing cysteine/homocysteine in living cells and daphnia magna model, Anal. Chem. 91 (2019) 12531–12537.
[4] C.X. Yin, K.M. Xiong, F.J. Huo, J.C. Salamanca, R.M. Strongin, Fluorescent probes with multiple binding sites for the discrimination of Cys, Hcy, and GSH, Angew. Chem. 129 (2017) 13368–13379.
[5] L.H. Zhai, Z.L. Shi, Y.Y. Tu, S.Z. Pu, A dual emission fluorescent probe enables simultaneous detection and discrimination of Cys/Hcy and GSH and its application in cell imaging, Dyes Pigm. 165 (2019) 164–171.
[6] X.B. Wang, H.J. Li, C. Liu, Y.X. Hu, M.C. Li, Y.C. Wu, Simple turn-on fluorescent sensor for discriminating Cys/Hcy and GSH from different fluorescent signals, Anal. Chem. 93 (2021) 2244–2253.
[7] L. Yang, Y.N. Su, Y.N. Geng, Y. Zhang, X.J. Ren, L. He, X.Z. Song, A triple-emission fluorescent probe for discriminatory detection of cysteine/homocysteine, glutathione/hydrogen sulfide, and thiophenol in living cells, ACS Sens. 3 (2018) 1863–1869.
[8] Y.F. Huang, Y.B. Zhang, F.J. Huo, J.B. Chao, F.Q. Cheng, C.X. Yin, A new strategy: distinguishable multi-substance detection, multiple pathway tracing based on a new site constructed by the reaction process and its tumor targeting, J. Am. Chem. Soc. 142 (2020) 18706–18714.
[9] L.W. He, Q.Y. Xu, Y. Liu, H.P. Wei, Y.H. Tang, W.Y. Lin, Coumarin-based turn-on fluorescence probe for specific detection of glutathione over cysteine and homocysteine, ACS Appl. Mater. Interfaces 7 (2015) 12809–12813.
[10] Y. Yang, Y. Feng, H. Li, R. Shen, Y.Z. Wang, X.R. Song, C. Cao, G.L. Zhang, W.S. Liu, Hydro-soluble NIR fluorescent probe with multiple sites and multiple excitations for distinguishing visualization of endogenous Cys/Hcy, and GSH, Sens. Actuators, B 333 (2021) 129189.
[11] K.M. Xiong, F.J. Huo, J.B. Chao, Y.B. Zhang, C.X. Yin, Colorimetric and NIR fluorescence probe with multiple binding sites for distinguishing detection of Cys/Hcy and GSH in vivo, Anal. Chem. 91 (2019) 1472–1478.
[12] Z.Y. Zhou, G.F. Duan, Y.Y. Wang, S.K. Yang, X.Y. Liu, L.Y. Zhang, R.N. Sun, Y.G. Xu, Y.Q. Gu, X.M. Zha, A highly sensitive fluorescent probe for selective detection of cysteine/homocysteine from glutathione and its application in living cells and tissues, New J. Chem. 42 (2018) 18172–18181.
[13] M. Li, X.M. Wu, Y. Wang, Y.S. Li, W.H. Zhu, T.D. James, A near-infrared colorimetric fluorescent chemodosimeter for the detection of glutathione in living cells, Chem. Commun. 50 (2014) 1751–1753.
[14] Z.X. Liu, X. Zhou, M. Yu, H. Ying, N. Kwon, X. Wu, J.Y. Yoon, A reversible fluorescent probe for real-time quantitative monitoring of cellular glutathione, Angew. Chem., Int. Ed. 129 (2017) 5906–5910.
[15] R. Huang, B.B. Wang, X.M. Situ, T. Gao, F.F. Wang, H. He, X.Y. Fan, F.L. Jiang, Y. Liu, A lysosome-targeted fluorescent sensor for the detection of glutathione in cells with an extremely fast response, Chem. Commun. 52 (2016) 11579–11582.
[16] Y.L. Zhang, X.M. Shao, Y. Wang, F.C. Pan, R. Kang, F.F. Peng, Z.T. Huang, W.J. Zhang, W.L. Zhao, Dual emission channels for sensitive discrimination of Cys/Hcy and GSH in plasma and cells, Chem. Commun. 51 (2015) 4245–4248.
[17] B.K. Rani, S.A. John, A novel pyrene based fluorescent probe for selective detection of cysteine in presence of other bio-thiols in living cells, Biosens. Bioelectron. 83 (2016) 237–242.
[18] K.B. Li, W.B. Qu, Q.X. Shen, S.Q. Zhang, W. Shi, L. Dong, D.M. Han, 1,8-Naphthalimide-based dual-response fluorescent probe for highly discriminating detection of Cys and H_2S, Dyes Pigm. 173 (2020) 107918.
[19] Y.K. Yue, F.J. Huo, P. Ning, Y.B. Zhang, J.B. Chao, X.M. Meng, C.X. Yin, Dual-site fluorescent probe for visualizing the metabolism of Cys in living cells, J. Am. Chem. Soc. 139 (2017) 3181–3185.
[20] H. Zhang, W.X. Li, J.L. Chen, G.F. Li, X.X. Yue, L.L. Zhang, X.Z. Song, W.Q. Chen, Simultaneous detection of Cys/Hcy and H_2S through distinct fluorescence channels, Anal. Chim. Acta 1097 (2020) 238–244.
[21] H.B. Fang, Y.C. Chen, Y.J. Wang, S.S. Geng, S.K. Yao, D.F. Song, W.J. He, Z.J. Guo, A dual-modal probe for NIR fluorogenic and ratiometric photoacoustic imaging of Cys/Hcy in vivo, Science China Chemistry 5 (2020) 699–706.
[22] X.Y. Qiu, X.J. Jiao, C. Liu, D.S. Zheng, K. Huang, Q. Wang, S. He, L.C. Zhao, X.S. Zeng, A selective and sensitive fluorescent probe for homocysteine and its application in living cells, Dyes Pigm. 140 (2017) 212–221.
[23] S. Xu, J.L. Zhou, X.C. Dong, W.L. Zhao, Q.G. Zhu, Fluorescent probe for sensitive discrimination of Hcy and Cys/GSH in living cells via dual-emission, Anal. Chim. Acta 1074 (2019) 123–130.
[24] Y.K. Yue, F.J. Huo, X.Q. Li, T. Yi, Y. Wen, J. Salamanca, J.O. Escobedo, R.M. Strongin, C.X. Yin, pH-dependent fluorescent probe that can be tuned for cysteine or homocysteine, Org. Lett. 19 (2017) 82–85.
[25] X.F. Song, Y.Y. Tu, R.J. Wang, S.Z. Pu, A lysosome-targetable fluorescent probe for simultaneous detection and discrimination of Cys/Hcy and GSH by dual channels, Dyes Pigm. 177 (2020) 108270.
[26] J. Liu, Y.Q. Sun, Y.Y. Huo, H.X. Zhang, L.F. Wang, P. Zhang, D. Song, Y.W. Shi, W. Guo, Simultaneous fluorescence sensing of Cys and GSH from different emission channels, J. Am. Chem. Soc. 136 (2014) 574–577.
[27] B. Yu, C.Y. Chen, J.X. Ru, W.F. Luo, W.S. Liu, A multifunctional two-photon fluorescent probe for detecting H_2S in wastewater and GSH in vivo, Talanta 188 (2018) 370–377.
[28] Y.Q. Tang, L.Y. Jin, B.Z. Yin, A dual-selective fluorescent probe for GSH and Cys detection: Emission and pH dependent selectivity, Anal. Chim. Acta 993 (2017) 87–95.
[29] Y.Y. Mao, Y.D. Xu, Z. Li, Y. Wang, H.H. Du, L. Liu, R. Ding, G.D. Liu, A GSH Fluorescent Probe with a Large Stokes Shift and Its Application in Living Cells, Sensors 19 (2019) 5348.
[30] Y. Tian, B.C. Zhu, W. Yang, J. Jing, X.L. Zhang, A fluorescent probe for differentiating Cys, Hcy and GSH via a stepwise interaction, Sens. Actuators, B 262 (2018) 345–349.
[31] R.F. McFeeters, A.O. Barish, Sulfite analysis of fruits and vegetables by high-performance liquid chromatography (HPLC) with ultraviolet spectrophotometric detection, J. Agric. Food Chem. 51 (2003) 1513–1517.
[32] J. Vacek, B. Klejdus, J. Petrlova, L. Lojkova, V. Kuban, A hydrophilic interaction chromatography coupled to a mass spectrometry for the determination of glutathione in plant somatic embryos, Analyst 131 (2006) 1167–1174.
[33] A.P. Vellasco, R. Haddad, M.N. Eberlin, N.F. Hoehr, Combined cysteine and homocysteine quantitation in plasma by trap and release membrane introduction mass spectrometry, Analyst 127 (2002) 1050–1053.
[34] Y. Li, W.M. Liu, P.P. Zhang, H.Y. Zhang, J.S. Wu, J.C. Ge, P.F. Wang, A fluorescent probe for the efficient discrimination of Cys, Hcy and GSH based on different cascade reactions, Biosens. Bioelectron. 90 (2017) 117–124.

[35] X.J. Ren, Y. Zhang, F. Zhang, H. Zhong, J.P. Wang, X.J. Liu, Z.G. Yang, X.Z. Song, Red-emitting fluorescent probe for discrimination of Cys/Hcy and GSH with a large Stokes shift under a single-wavelength excitation, Anal. Chim. Acta 1097 (2020) 245–253.
[36] Y.L. Fu, X.G. Chen, H. Li, W. Feng, Q.H. Song, Quinolone-based fluorescent probes for distinguished detection of Cys and GSH through different fluorescence channels, New J. Chem. 44 (2020) 13781–13787.
[37] P.Y. Wu, M. Jiang, X.F. Hu, J.R. Wang, G.J. He, Y. Shi, Y. Li, W. Liu, J. Wang, Amide-containing luminescent metal-organic complexes as bifunctional materials for selective sensing of amino acids and reaction prompting, RSC Adv. 6 (2016) 27944–27951.
[38] G.J. He, X.L. Liu, J.H. Xu, L.G. Ji, L.L. Yang, A.Y. Fan, S.J. Wang, Q.Z. Wang, Synthesis and application of a highly selective copper ions fluorescent probe based on the coumarin group, Spectrochim. Acta, Part A 190 (2018) 116–120.
[39] S. Ghosh, N. Roy, T.S. Singh, N. Chattopadhyay, Photophysics of a coumarin based Schiff base in solvents of varying polarities, Spectrochim. Acta, Part A 188 (2018) 252–257.
[40] B.L. Dong, Y.R. Lu, N. Zhang, W.H. Song, W.Y. Lin, Ratiometric imaging of cysteine level changes in endoplasmic reticulum during H_2O_2-induced redox imbalance, Anal. Chem. 91 (2019) 5513–5516.
[41] K. Anusuyadevi, S.P. Wu, S. Velmathi, ESIPT triggered swift determination of cysteine in HeLa cell line during redox imbalance, J. Photochem. Photobiol., A 403 (2020) 112875.
[42] A.N. Pham, G.W. Xing, C.J. Miller, T.D. Waite, Fenton-like copper redox chemistry revisited: Hydrogen peroxide and superoxide mediation of copper-catalyzed oxidant production, J. Catal. 301 (2013) 54–64.
[43] G.T. Sfrazzetto, C. Satriano, G.A. Tomaselli, E. Rizzarelli, Synthetic fluorescent probes to map metallostasis and intracellular fate of zinc and copper, Coord. Chem. Rev. 311 (2016) 125–167.
[44] N. Zhou, F.J. Huo, Y.K. Yue, K.Q. Ma, C.X. Yin, Rearrangement regulated cysteine fluorescent probe for cellular oxidative stress evaluation induced by copper (II), Chin. Chem. Lett. 11 (2020) 2970–2974.